A multicolor quantum dot intersublevel detector with photoresponse in the terahertz range

G. Huang, J. Yang, and P. Bhattacharya[a)]
Solid State Electronics Laboratory, Department of Electrical Engineering and Computer Science, University of Michigan, Ann Arbor, Michigan 48109-2122, USA

G. Ariyawansa and A. G. U. Perera
Department of Physics and Astronomy, Georgia State University, Atlanta, Georgia 30303, USA

(Received 25 October 2007; accepted 11 December 2007; published online 7 January 2008)

An $In_{0.4}Ga_{0.6}As/GaAs$ multi quantum-dot layer intersublevel detector with multicolor detection is demonstrated. The *n*-type doping in the dots is carefully adjusted during molecular beam epitaxy of the device heterostructure to control the dark current and the occupation of the dot states as a function of temperature. The device demonstrates several photoresponse peaks in the 3–13 and 20–55 μm (15–5.4 THz) ranges. At 150 K, the response in the terahertz range has a peak responsivity of 0.05 A/W and specific detectivity D^* of 2×10^7 Jones for an applied bias of −2 V. © *2008 American Institute of Physics*. [DOI: 10.1063/1.2830994]

The development of high power terahertz sources[1] and spectroscopic techniques such as terahertz time domain spectroscopy[2] have demonstrated the use of terahertz radiation (0.1–10 THz) for material characterization, chemical and biological sensing, submillimeter astronomy,[3] and several other applications.[4] At the present time, terahertz detectors (or receivers) used in aforementioned applications are Ge blocked impurity band detectors, photoconductors triggered by femtosecond laser pulses, and bolometers operating at low temperatures. These detector systems are complicated and bulky. Hence, for future terahertz technology, there is a need for compact, fast, high sensitive, and electronic terahertz detectors operating at high temperatures. One possible choice would be a quantum dot intersublevel photodetector (QDIP),[5] in which electronic transitions between energy states can lead to terahertz radiation detection.[6] Quantum dot-based detectors also exhibit multicolor characteristics, which can be used for multispectral detection capabilities.[7] Detecting an object's infrared (IR) emission at multiple wavelengths can be used to eliminate background effects and reconstruct the object's absolute temperature. This also plays an important role in differentiating the object from its background.

We report here a multicolor QDIP with response peaks in the 3–13 and 20–55 μm (15–5.4 THz) ranges and operating at temperatures up to 150 K. Ground-based IR detector applications involve detectors operating in two atmospheric windows (3–5 and 8–14 μm) of which the more useful range is 8–14 μm since 300 K blackbody emission (10 μm) falls in this region. For space surveillance and space situational awareness,[8] where extremely faint cold objects against a dark background have to be observed, multiband focal plane arrays operating in very long wavelength infrared (14–30 μm) are required. In astronomy, where infrared technology plays a dominant role in observing celestial objects, the midinfrared response (4–12 μm) of the detector can be used to observe cooler red objects and the far-infrared response (20–55 μm) is useful to detect cold objects such as comets, planets, and interstellar dust. Detectors sensitive in 3–14 and 20–50 μm are also useful for identification of protoplanetary nebulae[9] using their features in the emission spectrum.

Our objective was to demonstrate a QDIP with a simple quantum dot heterostructure in the active region, having strong photoresponse at relatively high temperatures at the two wavelength ranges of interest. We have, therefore, designed the device with multiple layers of $In_{0.4}Ga_{0.6}As/GaAs$ quantum dots. An eight-band $\mathbf{k}\cdot\mathbf{p}$ model was used to calculate the dot electronic states with the effects of strain included with the valence force field model.[10] The actual dot size is estimated from atomic force microscopy measurements on a dot ensemble. The quantum dots grown by molecular beam epitaxy (MBE) typically have near-pyramidal shape with an average base width of 21 nm and height of 5 nm. The calculated energy levels in these dots are shown schematically in Fig. 1(a). Also shown in the figure are the wavelengths of photons that can be absorbed by the dots due to intersublevel transitions, provided the initial states are filled with electrons. Thus, radiation corresponding to wavelengths ~8, 18, and 60 μm are expected to be absorbed, based on the calculations.

The $In_{0.4}Ga_{0.6}As/GaAs$ photoconductive QDIP heterostructure was grown by MBE on a (001)-oriented semi-insulating GaAs substrate. The active region consists of 20 $In_{0.4}Ga_{0.6}As/GaAs$ quantum dots layers separated by 500 Å thick GaAs layers. The dots and spacers were grown continuously at 500 °C. The quantum dots are *n* doped with silicon with an estimated doping level of 1 electron per dot. This doping level is very critical since it is essential to have electrons in the initial states for the various transitions at different temperatures. Silicon doped (2×10^{18} cm^{-3}) GaAs layers are grown below (0.8 μm) and above (0.2 μm) the active region to facilitate Ohmic contacts. Circular mesas for top illumination were fabricated by standard photolithography, wet chemical etching, and contact metallization techniques. The diameter of the circular illumination area is 600 μm. Devices for measurement are mounted on to chip carriers and gold wire contacts are made from individual devices to separate leads of the carrier. The chip carrier is mounted in a

a)Electronic mail: pkb@eecs.umich.edu.

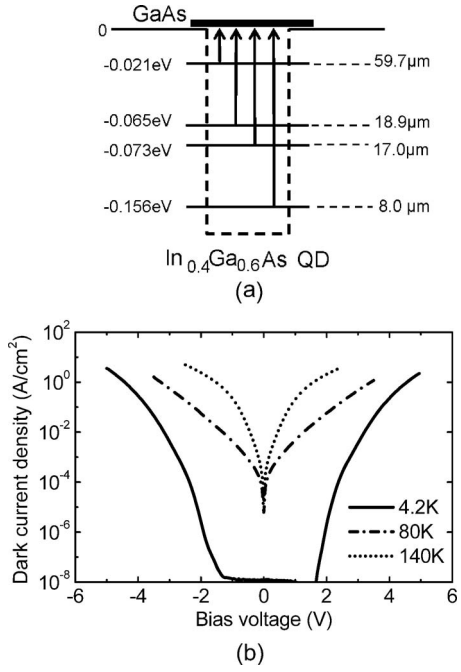

FIG. 1. (a) Electron energy levels in an $In_{0.4}Ga_{0.6}As/GaAs$ self organized quantum dot calculated with an eight-band $\mathbf{k}\cdot\mathbf{p}$ model. The shape of the dot was assumed to be pyramidal with base of 21 nm and height of 5 nm; (b) measured temperature-dependent dark current voltage characteristics of a QDIP with 600 μm diameter illumination area.

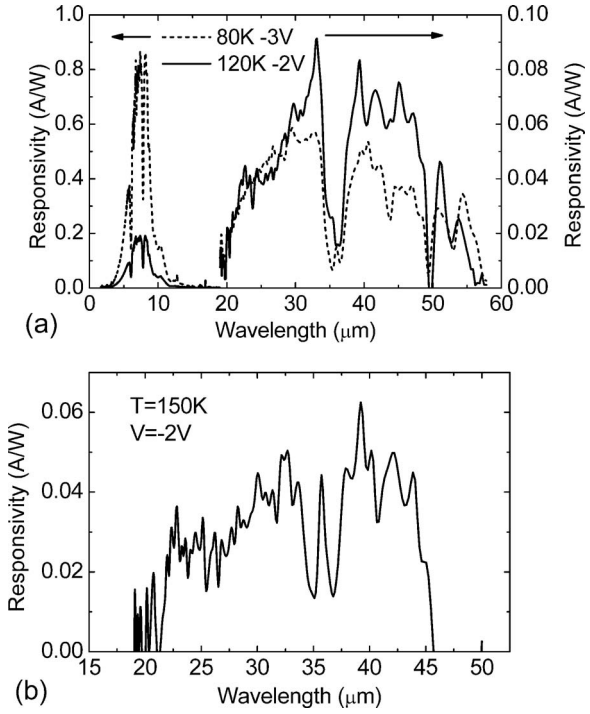

FIG. 2. Spectral responsivities of QDIPs measured at (a) 80 and 120 K and (b) 150 K.

variable temperature cryostat (4.2–300 K) for dark current and spectral response measurements. Several identical devices were measured and results obtained from the best one are reported here.

The measured temperature-dependent dark current-voltage characteristics of a typical device of mesa diameter 600 μm are shown in Fig. 1(b). The current densities at a bias of −2 V are 2.55×10^{-6}, 5.58×10^{-2}, and 1.17 A/cm^2 at 4.2, 80, and 140 K, respectively. We attribute the relatively low dark current to three-dimensional confinement in the quantum dots, optimized doping of the dots and the presence of the GaAs barrier layers. The dark current measurement is used to examine the spatial uniformity of the fabricated devices and to calibrate the spectral response.

The normal incidence spectral responses, both in midinfrared and far-infrared regions, were obtained using a System 2000 Perkin Elmer Fourier transform infrared spectrometer and a globar broadband source. Different beam splitters and dewar windows specific to mid-infrared and far-infrared (FIR) were used in the measurements. The calibration was performed by using the spectra obtained from a Si composite bolometer with a known sensitivity with the same set of optical components. The calibrated spectral response of the QD photodetector at 80 and 120 K with biases of −3 and −2 V, respectively, is shown in Fig. 2(a). Two response peaks are observed in the ranges of 3–13 and 20–55 μm. The response in the 3–13 μm range is centered at ~8 μm and has peak responsivities of 0.86 and 0.19 A/W at 80 and 120 K, respectively. The response from 20–55 μm is fairly broad with peak responsivities of 0.05 and 0.08 A/W at 80 and 120 K, respectively. The center of the peak is around 40 μm. The sharp drop centered at ~36 μm is due to longitudinal optical phonon absorption in GaAs, which has been reported in other experiments.[11,12] Figure 2(b) shows the measured and calibrated responsivity at 150 K for an applied bias of −2 V. The peak responsivity at ~40 μm is still as high as 0.05 A/W. These devices, therefore, offer the potential for high temperature terahertz detection.

In comparing the measured spectral response with the calculated energies of the bound electron energy levels in the quantum dot, shown in Fig. 1(a), it is apparent that the response peaking at ~8 μm corresponds to a transition of electrons from the ground state to the continuum. We believe that the photoresponse peak at ~40 μm results from transitions from the highest dot excited states to the continuum. The reasons why the observed peak at ~40 μm does not match exactly with the calculated excited state level (59.7 μm) are (a) the nonuniformity in the dot size broadens the response peaks; and (b) for eight band $\mathbf{k}\cdot\mathbf{p}$ calculations, energy levels close to the band edge always have larger errors than levels far from the band edge. A shoulder to the FIR peak at ~22 μm is distinctly seen in the data of Figs. 2(a) and 2(b) and this feature becomes more prominent at higher temperatures. Again, we believe this peak results from transitions from the second excited states to the continuum.

Further evidence of the origin of the peaks is provided by the temperature dependence of the peak responsivity, which is illustrated in Fig. 3. From 80 to 120 K, the peak responsivity of the 8 μm absorption peak decreases by ~80%, while the peak responsivity of the 40 μm transition increases by a factor of 6 when the temperature increases from 4 to 120 K. These trends can be accounted for by considering the thermal excitation of carriers from the ground state to excited states. Even the peak responsivity of the 22 μm transition decreases from 0.04 to 0.03 A/W, possibly due to thermal excitation from the second to higher excited states, as the temperature is increased from 120 to 150 K.

The specific detectivity (D^*), which is a measure of the signal-to-noise ratio of the device, was calculated from the measured peak responsivity R_p and noise density spectra S_i at different temperatures and applied biases. The noise spectra

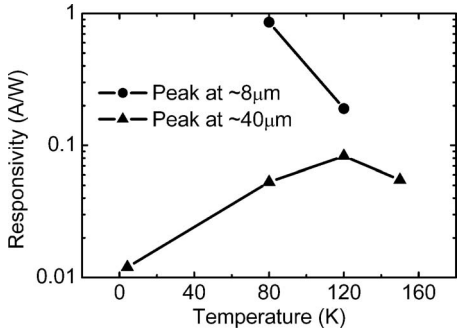

FIG. 3. Variation of measured peak responsivity with temperature for absorption with peaks at 8 and 40 μm.

were measured with a dual channel fast fourier transform signal analyzer and a low noise preamplifier. A thick copper plate was used as a radiation block to provide the dark conditions for the measurements. The specific detectivity is calculated from $D^*=R_pA^{1/2}/S_i^{1/2}$. The values of D^* for the 8 μm peak are 2×10^9 Jones at 80 K (−3 V bias) and 7.2×10^7 Jones at 120 K (−2 V). For the 40 μm peak the values of D^* are 1.3×10^8 Jones at 80 K (−3 V), 2.8×10^7 Jones at 120 K (−2 V) and 2×10^7 Jones at 150 K (−2 V). The D^* value for the 8 μm peak are lower than the best values that we and others have measured in the past[13–15] and this is attributed to the higher dark current in these devices due to a higher doping level. However, the D^* value for the terahertz absorption transition are larger than those reported earlier.

In conclusion, we demonstrate a multicolor QDIP with a simple quantum dot heterostructure absorption region. The device exhibits strong absorption peaks in the 3–13 and 20–55 μm ranges with large responsivity and detectivity at temperatures up to 150 K. By tuning the dot size, alloy composition, and barrier layer bandgap, it should be possible to extend the terahertz absorption into the 1–3 THz range.

The work was supported by the Air Force Office of Scientific Research under Grant No. FA9550-06-1-0500 and the National Science Foundation under Grant No. ECS-0620688.

[1]B. Ferguson and X.-C. Zhang, Nat. Mater. **1**, 26 (2002).
[2]B. B. Hu and M. C. Nuss, Opt. Lett. **20**, 1716 (1995).
[3]T. G. Phillips and J. Keene, Proc. IEEE **80**, 1662 (1992).
[4]P. H. Siegel, IEEE Trans. Microwave Theory Tech. **50**, 910 (2002).
[5]J. Phillips, P. Bhattacharya, S. W. Kennerly, D. W. Beekman, and M. Dutta, IEEE J. Quantum Electron. **35**, 936 (1999).
[6]X. H. Su, J. Yang, P. Bhattacharya, G. Ariyawansa, and A. G. U. Perera, Appl. Phys. Lett. **89**, 031117 (2006).
[7]S. Krishna, S. Raghavan, G. von Winckel, A. Stintz, G. Ariyawansa, S. G. Matsik, and A. G. U. Perera, Appl. Phys. Lett. **83**, 2745 (2003).
[8]P. M. Alsing, D. A. Cardimona, D. H. Huang, T. Apostolova, W. R. Glass, and C. D. Castillo, Infrared Phys. Technol. **50**, 89 (2007).
[9]P. García-Lario, A. Manchado, A. Ulla, and M. Manteiga, Astrophys. J. **513**, 941 (1999).
[10]H. Jiang and J. Singh, Phys. Rev. B **56**, 4696 (1998).
[11]H. Luo, H. C. Liu, C. Y. Song, and Z. R. Wasilewski, Appl. Phys. Lett. **86**, 231103 (2005).
[12]D. G. Esaev, M. B. M. Rinzan, S. G. Matsik, A. G. U. Perera, H. C. Liu, B. N. Zvonkov, V. I. Gavrilenko, and A. A. Belyanin, J. Appl. Phys. **95**, 512 (2004).
[13]S. Chakrabarti, A. D. Stiff-Roberts, P. Bhattacharya, S. Gunapala, S. Bandara, S. B. Rafol, and S. W. Kennerly, IEEE Photonics Technol. Lett. **16**, 1361 (2004).
[14]S. Krishna, D. Forman, S. Annamalai, P. Dowd, P. Varangis, T. Tumolillo, A. Gray, J. Zilko, K. Sun, M. Liu, J. Campbell, and D. Carothers, Phys. Status Solidi C **3**, 439 (2006).
[15]E. Kim, A. Madhukar, Z. Ye, and J. C. Campbell, Appl. Phys. Lett. **84**, 3277 (2004).